

TROPOSPHERIC REFRACTION AND ITS INFLUENCE THROUGH ZENITH TOTAL PATH DELAY AT DIFFERENT IGS STATIONS

Violeta Vasilic¹, Ljiljana Brajovic², Dušan Petković¹, Dragan Blagojević¹*

¹University of Belgrade, Faculty of Civil Engineering, Department of Geodesy and Geoinformatics, Belgrade, Republic of Serbia; e-mail: tatic@grf.bg.ac.rs; dpetkovic@grf.bg.ac.rs; bdragan@grf.bg.ac.rs

²University of Belgrade, Faculty of Civil Engineering, Department of Mathematics, Physics and Descriptive Geometry, Belgrade, Republic of Serbia; e-mail: brajovic@grf.bg.ac.rs

Abstract: The propagation of the Global Navigation Satellite System (GNSS) signals through the atmosphere is affected by the electron content in the ionosphere and the air density in the electrically neutral troposphere, thus causing a signal delay and leading to errors in the GNSS observations and the estimated positions. Our research has been conducted related to the influence of the tropospheric layer of the Earth's atmosphere on signals at geodetic observation stations in the zenith direction. Since tropospheric refraction cannot be directly estimated, the signal delay has been quantified by applying several developed models. As the lowest layer of the atmosphere, the average height of the troposphere is approximately ten kilometers, and it is variable concerning the latitude of the measuring station and seasonal conditions. The tropospheric delay of the GNSS signal - Zenith Total Delay (ZTD), was analyzed on the examples of three International GNSS Service (IGS) stations at different latitudes. Two epochs in July 2022 and January 2023 for each IGS station are considered regarding seasonal differences in the atmospheric parameters. It was found that at each of the IGS stations, there is an oscillation of the ZTD amplitude with a half-day period. Different patterns were distinguished at each station, depending on the station latitude and epoch, i.e., summer or winter atmospheric conditions. For example, a random walk signal was dominant at the ROAG, San Fernando IGS station.

Keywords: IGS station; ZTD; GNSS signal

1. Introduction

The characteristics of the atmosphere's natural structure are variable in both space and time. Depending on them, the propagation of GNSS signal through the atmosphere is differently affected, and it is reflected in signal delay. High accuracy in the estimated positions of the geodetic stations will be enabled with appropriate modeling or with the reduction of signal delay errors. A simplified atmosphere model in the form of concentric layers of different heights is used to determine atmospheric parameters.

The lowest layer of the atmosphere is the troposphere, and according to Saastamoinen's model (Saastamoinen, 1972a, 1972b), the troposphere is the layer of the Earth's atmosphere with an average height of 10 km with a rate of temperature decrease of 6.5 degrees Celsius/km. Above the tropospheric layer, from the tropopause is a stratospheric layer with an average height of 70 km, in which the temperature is assumed to be constant.

*Corresponding author, e-mail: tatic@grf.bg.ac.rs

The analysis of ZTD of the GNSS signal was performed on the examples of three IGS stations at different latitudes METG, METSAHOVI, Finland, GOP6, ONDREJOV, Czechia and ROAG, SAN FERNANDO, Spain, for two epochs in July 2022 and January 2023. ZTD 5 min time series were downloaded from the NASA website (n.d.). This analysis has been performed regarding seasonal differences in the atmospheric parameters.

2. Theoretical aspects of ZTD and applied estimation models

At the zenith of GNSS stations, the tropospheric refraction is about 2.3 m, and the delay for signals closer to the horizon can be up to seven times higher. The basic mathematical expression of the correction for atmospheric refraction (Saastamoinen, 1972a, 1972b) in a spherically layered atmosphere is:

$$\Delta z = \int_1^{n_1} \frac{\tan z}{z} dn; (0 \leq z_1 \leq 90^\circ) \quad (1)$$

Solving the integral of atmospheric refraction, the refractive index function n is expanded following the trigonometric function of the zenith distance z , that the equation for obtaining ZTD according to Saastamoinen (1972a, 1972b) has the following form:

$$\rho = 0.002277 \cdot \frac{\left(P_0 + \left(0.05 + \frac{1255}{T_0 + 273.15} \right) e_0 \right)}{f(\varphi, h)} \quad (2)$$

$$e_0 = r_h \cdot 6.11 \cdot 10^{\frac{7.5 \cdot T_0}{T_0 + 273.3}}$$

$$f(\varphi, h) = 1 - 0.00266 \cdot \cos 2\varphi - 0.00028 \cdot h$$

where ρ denotes the ZTD, P_0 , T_0 , e_0 , and r_h denote the pressure, the temperature, the water vapor pressure, and the relative humidity, respectively, $f(\varphi, h)$ is the correction of gravity acceleration caused by the rotation of the Earth, φ denotes the latitude of the point, and h denotes the height, with the subscript 0 indicates the values of the parameters at the earth surface.

In addition to the Saastamoinen model, several models are used for modeling the tropospheric delay, such as the Hopfield model, the Herring model, and others. Tropospheric delay is generally considered the sum of two components: the tropospheric hydrostatic part or ZHD and the tropospheric wet part or ZWD (Blagojević, 2014; Cui et al., 2022). The hydrostatic component has a larger amplitude and contributes 90% to the total Zenith Total Delay, while the remaining portion is associated with the ZWD component. In the paper of authors Bevis et al. (1992), it is emphasized that according to most theorists, global warming will cause systematic changes in the total water vapor content of the atmosphere. In the paper of authors Labib et al. (2018), research on tropospheric delay related to different climate zones is presented.

The analysis of the ZTD time series was performed as follows. First, the linear trend was removed according to the model $y = a + bx$, and after that, the Fourier transformation was applied to the ZTD time series. Then ZTD time series were modeled using a fitting modeling function representing the sum of 8 sinusoidal oscillations. This fit function is used to approximate the time series and has the following form: $y(t) = A_1 \sin(2\pi f_1 t + \varphi_1) + A_2 \sin(2\pi f_2 t + \varphi_2) + \dots + A_8 \sin(2\pi f_8 t + \varphi_8)$, with the following notations: $y(t)$ is the value of the time series at time t , A_1 – A_8 are the amplitudes of the sinusoidal components, f_1 – f_8 are the frequencies of the corresponding sinusoidal components, and φ_1 – φ_8 are the phases of the corresponding sinusoidal components.

This fit function is used to explain ZTD's periodicity as well as allows the modeling and analysis of oscillations in the time series. Also, we have applied the autoregressive model of order 1 (AR (1)), $y(t) = c + \phi \cdot y(t-1) + \varepsilon(t)$, with the following notations: $y(t)$ is the current value, $y(t-1)$ is the previous value, ϕ is the autocorrelation coefficient at lag 1, c is a constant, and $\varepsilon(t)$ is white noise (Information technology laboratory, n.d.).



Figure 1. Spatial distribution and corresponding FFT of ZTD of IGS stations METG, GOP6, ROAG for July 2022 (left) and January 2023 (right).

3. The main ZTD characteristics of IGS stations in July 2022 and January 2023

The Fourier transformations of the ZTD time series for both epochs, July 2022 and January 2023, for all three stations are visually represented in Figure 1. They are listed in Table 1 with their main station data. ZTD time series with the modeled fit lines for both epochs are shown in Figure 2 for all three stations: METG, GOP6, and ROAG.

Table 1. The main characteristics of IGS stations

IGS station	Longitude	Latitude	Height
METG, METSAHOVI, Finland	24° 23' 03.0"	60° 14' 31.1"	59.7 m
GOP6, ONDREJOV, Czechia	14° 47' 08.2"	49° 54' 49.2"	592.6 m
ROAG, SAN FERNANDO, Spain	353° 47' 37.4"	36° 27' 48.1"	83.2 m

The shorter periods less than six days at station METG and less than five days at station GOP6, in both epochs, July and January, are approximately equal but have different amplitudes, indicating uniformity in periods across both epochs. Due to the convergence of the fit model for the July 2022 epoch at station GOP6, ZTD time series modeling was performed with 12 sinusoidal functions. In the case of station ROAG, the daily and semi-daily periods are the same and have approximately equal amplitudes in epochs July 2022 and with a slight difference in January 2023, while other periods with their appropriate amplitudes differ (Table 2). In July 2022, this station exhibited more oscillations with periods shorter than five days than in January 2023.

We estimated that ϕ autocorrelation coefficient at lag 1 is close to 1, and c constant term is zero for all ZTD time series. As the coefficient ϕ was slightly less than 1, we concluded that the ZTD time series exhibited exponential decay. The value of the autocorrelation coefficient at station ROAG in January 2023 was closest to 1, suggesting that a random walk-like type of signal was dominant. Based on their research, the authors Young et al. (2022), indicate the regional variability of the optimal random walk per station, which is determined by climatic, geographical, and weather factors.

The parameter values of several characteristic oscillations for three IGS stations in July 2022 indicate that the maximum amplitudes with their appropriate periods decrease with decreasing of the station's latitudes and are for station METG: 0.03166 m (period 11.30 days), station GOP6: 0.01635 m (period 7.94 days), and station ROAG: 0.01363 m (period 15.09 days) (Table 2). The amplitudes with approximately a three-day period increase with decreasing latitudes and increasing station heights. The smallest amplitude at station METG is less than 5 mm, while the largest amplitude at station GOP6, which has the greatest height, is less than 10 cm, while at station ROAG, it has an amplitude less than 2 cm. The amplitudes with daily periods increase with decreasing latitude and increasing station height, so the smallest amplitude value for station METG is approximately 1 mm, and the largest for station GOP6 is approximately 5 mm. The semi-diurnal amplitude values are approximately the same as the daily values, except for station METG, which has a value of approximately 3 mm. The obtained standard deviations of residuals for all three stations are less than 2 cm. The parameter values of several characteristic oscillations for three IGS stations in January 2023 indicate that the maximum amplitudes with their appropriate periods decrease with decreasing latitudes of the stations.

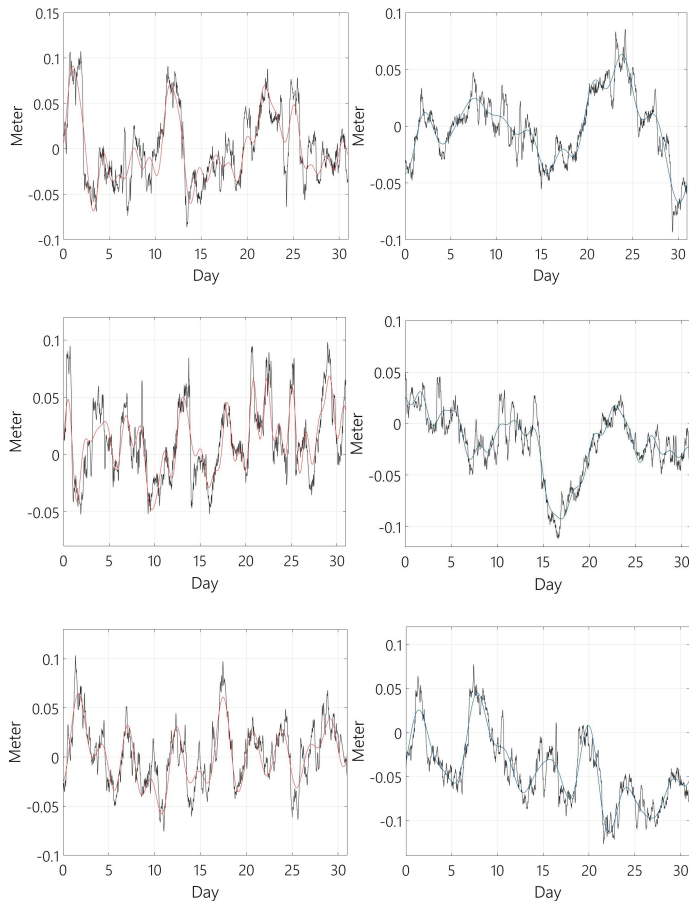


Figure 2. ZTD in July 2022 (left) and January 2023 (right) of IGS stations METG, GOP6, ROAG, and sine modeled lines.

Table 2. ZTD values of IGS stations for July 2022 and January 2023 concerning maximum amplitudes and approximately equal periods

IGS station	METG, July 2022				METG, January 2023			
Amplit. (m)	0.031656	0.001175	0.000928	0.003186	0.031859	0.003272	0.002486	0.000548
Period (day)	11.30	3.40	1.00	0.50	15.75	3.12	1.00	0.50
Phase (deg)	69.41	27.12	290.8782	291.28	263.22	268.85	5.68	103.09
IGS station	GOP6, July 2022				GOP6, January 2023			
Amplit. (m)	0.01635	0.09561	0.004723	0.00469	0.012153	0.00288	0.000462	0.001497
Period (day)	7.94	2.96	1.00	0.50	10.31	3.10	1.00	0.50
Phase (deg)	195.32	97.57	268.74	268.16	84.99	302.54	28.70	57.23
IGS station	ROAG, July 2022				ROAG, January 2023			
Amplit. (m)	0.013634	0.014301	0.004037	0.004533	0.010698	0.008588	0.001197	0.003596
Period (day)	15.09	2.81	1.00	0.50	11.01	3.10	1.00	0.50
Phase (deg)	51.21	319.50	210.20	208.99	81.25	245.52	245.44	114.66

Their values are as follows for station METG: 0.03186 m (period 15.75 days), station GOP6: 0.01215 m (period 10.31 days), and station ROAG: 0.01070 m (period 11.10 days). The amplitudes with a three-day period at stations METG and GOP6 are approximately equal and less than 5 mm, while the amplitude value for station ROAG is less than 1 cm. The amplitudes with daily periods decrease with decreasing latitude and increasing station height, so the smallest amplitude value for station GOP6, which has the greatest height, is 0.5 mm. Regarding semi-diurnal amplitude values, they increase with decreasing latitude of the station (Table 2). The obtained standard deviations of residuals for all three stations are less than 1.5 cm.

4. Conclusion

We have analyzed ZTD in two epochs in July 2022 and January 2023 of three IGS stations at different latitudes, and consequently of seasonal differences of the atmospheric parameters. At each IGS station, there are several oscillations of the ZTD amplitude with approximately three days, one-day, and half-day periods in both epochs. The values of maximum amplitudes and their periods differed in relation to summer or winter atmospheric conditions for all stations. This analysis could be useful in future investigations of the ZTD time series for an annual time period.

Acknowledgments

The Serbian Ministry of Science, Technological Development and Innovations, grant No. 200092, has supported the conducted research.

References

- Bevis, M., Businger, S., Herring, T. A., Rocken, C., Anthes, R. A., & Ware, R. H. (1992). GPS Meteorology: Remote Sensing of Atmospheric Water Vapor Using the Global Positioning System. *Journal of Geophysical Research: Atmospheres*, 97(D14), 15787–15801. <https://doi.org/10.1029/92JD01517>
- Blagojević, D. (2014). *Uvod u satelitsku geodeziju*. Građevinski fakultet Univerziteta u Beogradu.
- Cui, B., Wang, J., Li, P., Ge, M., & Schuh, H. (2022). Modeling wide-area tropospheric delay corrections for fast PPP ambiguity resolution. *GPS Solutions*, 26, Article 56. <https://doi.org/10.1007/s10291-022-01243-1>
- Information technology laboratory. (n.d.). *NIST/SEMATECH e-Handbook of Statistical Methods*. <http://www.itl.nist.gov/div898/handbook/>, date.
- Labib, B., Yan, J., Barriot, J.-P., Zhang, F., Feng, P. (2018). Monitoring Zenithal Total Delays over the three different climatic zones from IGS GPS final products: A comparison between the use of the VMF1 and GMF mapping functions. *Geodesy and Geodynamics*, 10(2), 93–99. <https://doi.org/10.1016/j.geog.2018.11.005>
- NASA. (n.d.). *ZTD 5 min time series*. <https://urs.earthdata.nasa.gov/home>
- Saastamoinen, J. (1972a). Atmospheric Correction for the Troposphere and Stratosphere in Radio Ranging of Satellites. In S. W. Henriksen, A. Mancini, & B. H. Chovitz (Eds.), *Use of Artificial Satellites for Geodesy* (pp. 247–251). American Geophysical Union. <https://doi.org/10.1029/GM015p0247>
- Saastamoinen, J. (1972b). Contributions to the theory of atmospheric refraction, *Bulletin Géodésique*, 105, 279–298, <https://doi.org/10.1007/BF02521844>
- Young, Z., Geoffrey, B., & Kreemer, C. (2022, December 12–16). *Application of Variable Random Walk Process Noise to Improve GPS Tropospheric Path Delay Estimation and Positioning at Local and Global Scales*. AGU22 fall meeting, Chicago IL, <https://agu.confex.com/agu/fm22/meetingapp.cgi/Paper/1162048>